NANO LETTERS

pubs.acs.org/NanoLett Letter

Large Enhancement of Critical Current in Superconducting Devices by Gate Voltage

Mirko Rocci,*,◆ Dhavala Suri,*,◆ Akashdeep Kamra, Gilvânia Vilela, Yota Takamura, Norbert M. Nemes, Jose L. Martinez, Mar Garcia Hernandez, and Jagadeesh S. Moodera*

Cite This: *Nano Lett.* 2021, 21, 216−221 Read Online

ABSTRACT: Significant control over the properties of a high-carrier density superconductor via an applied electric field has been considered infeasible due to screening of the field over atomic length scales. Here, we demonstrate an enhancement of up to 30% in critical current in a back-gate tunable NbN micro- and nano superconducting bridges. Our suggested plausible mechanism of this enhancement in critical current based on surface nucleation and pinning of Abrikosov vortices is consistent with expectations and observations for type-II superconductor films with thicknesses comparable to their coherence length. Furthermore, we demonstrate an applied electric field-dependent infinite electroresistance and hysteretic resistance. Our work presents an electric field driven enhancement in the superconducting property in type-II superconductors which is a crucial step toward the understanding of field-effects on the fundamental properties of a superconductor and its exploitation for logic and memory applications in a superconductor-based low-dissipation digital computing paradigm.

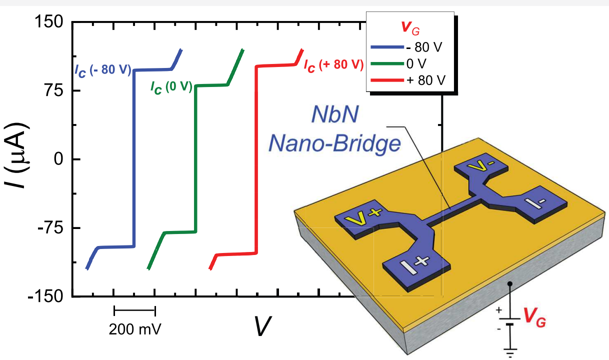

KEYWORDS: *NbN, Superconducting nanobridges, Gate tunability, Critical current, Electroresistance, Vortices*

INTRODUCTION

Semiconductor-based field-effect transistors (FETs), which have been instrumental in the silicon revolution, operate through modulation of resistance between the source and drain electrodes via an applied gate voltage. This modulation, in turn, is achieved via a change in the charge carrier density resulting from the electric field generated by the gate voltage. The relatively low carrier densities in semiconductors allow for a strong resistance modulation with reasonable gate voltages thereby enabling broad functionalities. Such a field effect is not expected to work with metals, which have a very high charge density compared to what can be induced by a gate voltage, and was shown to be negligibly weak.[1,2]

Gate-voltage modulation of superconductivity is considered immensely useful and has been attempted for some time,[3−6] including the recent advances in gate tunability of superconductivity in van der Waals materials.[7−9] Conventional superconductors have been amenable to control via interaction with magnetic fields[10−15] but not electric fields. Superconducting properties, such as critical temperature T_c of metallic superconductors, were found to be fairly insensitive to gate voltages,[3,16] exhibiting a minuscule change of $\sim 10^{-3}$%. In contrast, unconventional superconductors based on strongly correlated oxides allow for an efficient gate-modulation due to their relatively low carrier concentration.[4−6] The change in density of states at the chemical potential, which is associated with the gate-modulated carrier density, alters the superconducting order parameter and qualitatively explains the experimental observations discussed above.[6,16] This implies that superconducting properties, such as T_c, can be enhanced (reduced) by an increase (decrease) in the carrier concentration via a positive (negative) gate voltage. The change in superconducting properties is thus odd in the gate voltage, that is, "unipolar". Besides this quasi-equilibrium modulation, various nonequilibrium approaches to controlling the superconducting properties using electromagnetic radiation have been successful with significant advances demonstrated recently.[17,18]

In contrast with previous literature and expectations,[16,19] De Simoni and co-workers recently reported a gate-voltage-induced suppression of the critical current (I_c) in all-metallic superconducting nanobridges and junctions.[20−23] Furthermore, the observed suppression is even in the gate voltage, that is, "bipolar". Apart from the technological potential, these observations have raised two fundamental questions regarding

Received: September 2, 2020
Revised: November 25, 2020
Published: December 4, 2020

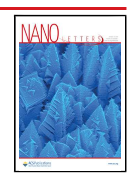

https://dx.doi.org/10.1021/acs.nanolett.0c03547
Nano Lett. 2021, 21, 216−221

(i) how a gate-voltage-induced electric field can affect a high-carrier density superconductor,[3,16,19,24,25] and (ii) what mechanism causes a change in the I_c. These crucial issues remain unaddressed thus far, although the possibility of the creation of metallic puddles,[26] which could reduce the I_c, has been floated. Various other mechanisms that may degrade superconductivity could be envisaged as accounting for the observed I_c reduction, for instance, injection of high-energetic carriers as established by the two most recent experiments with compelling evidence considering the size of leakage currents.[27,28]

Here, we demonstrate a bipolar gate-voltage-induced "enhancement" in the I_c of NbN (high carrier density superconductor) based superconducting bridges by 30%, whereas the critical temperature remains insensitive to the applied voltage. Besides uncovering novel fundamental phenomena, we demonstrate infinite electroresistance, that is, gate-voltage-controlled change in resistance between zero and a finite value, and hysteretic resistance variation versus gate voltage. These two effects could be exploited for low-dissipation logic and memory elements based on superconductors. We further demonstrate that the observed phenomena work for bridges in the nanoscale providing a proof-of-principle for scalability of such a technological paradigm. We also qualitatively discuss a plausible mechanism for the observed critical current modulation with the gate voltage. Hypothesizing that the critical current in our films is the value at which flux creep from one edge to the other becomes energetically favorable[29,30] by overcoming Bean-Livingston surface barrier,[31] a gate-voltage-induced enhancement of this surface barrier could account for our experiments and is consistent with related literature.[29,30,32−35] Altogether, our work provides crucial insights for understanding the field effect in metallic superconductors demonstrating that it could be further optimized with suitable surface termination and employed for enhancing, instead of suppressing, superconducting properties.

Synthesis and Fabrication. Niobium nitride (NbN) thin films with thicknesses t = 10 and 7 nm were grown on Si/SiO_2 substrates (Figure 1). The 300 nm thick SiO_2 layer ensured electrical isolation between the superconducting film and the p-doped Si substrate acting as the gate. NbN thin films with Al_2O_3 (t = 5 nm) capping were grown in situ by reactive DC magnetron sputtering (for NbN) and by standard RF nonreactive magnetron sputtering (for Al_2O_3). Substrates were annealed at 573 K for 1 h in UHV prior to the deposition. The base pressure of the sputtering chamber before the film deposition was below 5×10^{-8} Torr. The thin film growth was found to be polycrystalline in texture with sharp, well-defined NbN characteristic peaks in X-ray diffraction spectrum (see Supporting Information). The multilayer structures were then patterned via e-beam lithography into a microbridge (μB) with length l = 10 μm, width w = 1 μm, and thickness t = 10 nm, and a nanobridge (NB) with l = 1 μm, w = 100 nm, and t = 7 nm (Figure 1). Negative-tone resist was spun on the film and exposed at 10 kV following a soft bake. The resulting pattern was developed and the samples were then Ar^+ ion-milled to fabricate the bridges.

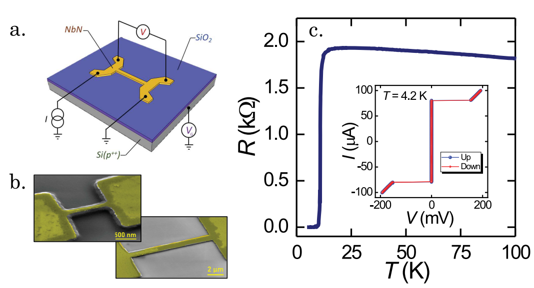

Figure 1. NbN device schematics and characterization. (a) Schematic depicting the measurement geometry of NbN bridges. (b) Pseudo-color scanning electron micrographs [image taken with sample tilted by 55°] of the fabricated 100 nm wide NB [left] and 1 μm wide μB [right]. (c) Resistance versus temperature variation for the μB device showing the superconducting transition at ∼10.8 K. Inset shows current−voltage characteristics of the device at 4.2 K (for both forward and backward scans).

■ RESULTS

We first present our experiments on the μB device. It was cooled down below its transition temperature into the superconducting state. A transition temperature $T_c \approx 10.8$ K can be seen in the temperature dependence of resistance shown in Figure 1c, similar to previous NbN thin films, (for example, ref 36). The inset depicts the corresponding $I-V$ characteristics at 4.2 K showing an I_c of about 82.5 μA. The Bardeen−Cooper−Schrieffer (BCS) energy gap $2\Delta_0 = 4.05\, k_B T_c$ corresponds to ∼4.16 meV, where k_B is the Boltzmann constant.[37,38] The London penetration depth is derived from the above parameters as $\lambda_L = \sqrt{\hbar R_N wt/\pi\mu_0 l\lambda_0} \approx 450$ nm, where l = 10 μm, w = 1 μm, and t = 10 nm are length, width, and thickness of the bridge, respectively. R_N = 2 kΩ is the resistance in the normal state at low temperature, and μ_0 is magnetic permeability in vacuum. The Ginzburg−Landau coherence length is estimated as $\xi_{GL} = \sqrt{\hbar l/R_N wtN_F e^2\Delta_0} \approx 9$ nm, where $N_F = 1.65 \times 10^{28}/(m^3\ eV)$ is the density of states in NbN at the Fermi level,[39] and e is the electronic charge. This places the Pearl length[40,41] $(2\lambda_L^2/t)$ at around 40 μm ($\gg w$) ensuring a spatially uniform current through the film.

Further, the same μB was investigated for its electric field response by applying back-gate voltage as depicted in Figure 1a. Figure 2a shows current−voltage characteristics of the μB at different back-gate voltages (V_G varying from −80 V to +80 V) at 4.2 K. The I_c enhances with the increase in gate voltage from ∼80 to 105 μA (i.e., an increase in critical current density, J_c from 0.80×10^6 to 1.03×10^6 A cm^{-2}). The enhancement shows a nearly symmetric response with respect to the gate voltage polarity [Figure 2b] and is observed to be ∼30% which is the largest modulation to date.[20] The applied voltage, however, did not produce any observable change in the critical temperature. As discussed below, the observed enhancement in the I_c, as compared to the previously reported suppression,[20] may be attributed to our choice of superconductor (type II) and the film thickness that is comparable to the superconducting coherence length.

Next, we examine the resistance variation with gate voltage (Figure 2c) biasing the device at a constant current of 85 μA. The device completely recovers the superconducting state from the normal state for a finite value of gate voltage <20 V. This modulation of resistance may be used to define an "electroresistance" ER, similar to the well-known magnetoresistance,[42−45] ER ≡ $(R_{max} - R_{min})/R_{min}$, which yields infinite value for our μB. The response is symmetric with respect to gate voltage polarity and is a direct consequence of the gate-

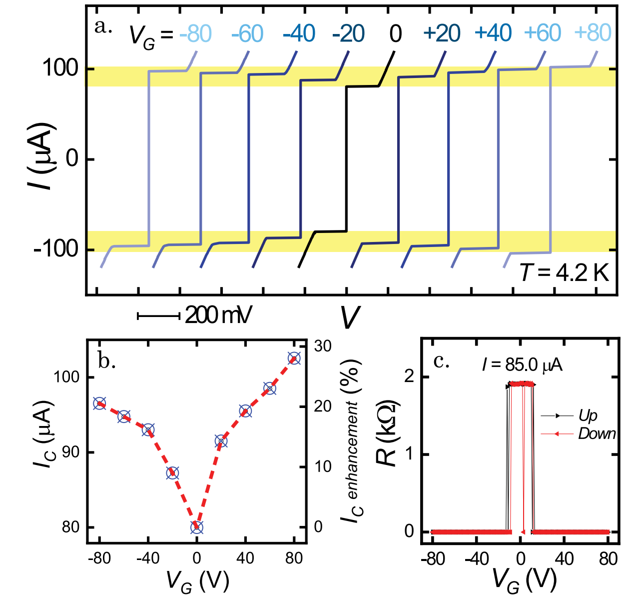

Figure 2. Gate-voltage-control of the μB properties at 4.2 K. (a) Current−voltage characteristics for various values of the back-gate voltage V_G. (b) I_c as a function of back-gate voltage. Scale on the right shows the corresponding enhancement percentage. (c) Resistance of μB as a function of back gate voltage at a constant current bias of 85 μA.

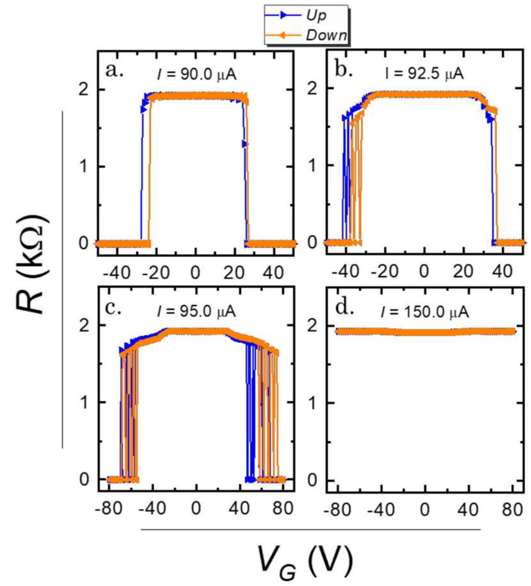

Figure 3. Back-gate-controlled switching between superconducting and normal states at different bias currents at 4.2 K. Resistance of the μB as a function of back-gate voltage for bias currents of (a) 90 μA, (b) 92.5 μA, (c) 95 μA, and (d) 150 μA. Both forward and backward sweeps are shown.

voltage-induced I_c enhancement. We rule out the possibility of such a response as being due to heating or electronic refrigeration effects as mentioned in ref 46 by noting that the measurements were performed by immersing the sample in liquid helium in a storage dewar. This helps maintain the sample in thermodynamic equilibrium. We also remark that the leakage current due to the applied electric field was ≤1 nA. Any spurious effect due to gate leakage can be ruled out as it would only lead to a reduction in critical current.

We also study electric field-induced switching of the device by applying different bias currents (90, 92.5, 95, and 150 μA) as shown in Figure 3. The back-gate voltage was scanned for both upward (negative to positive) and downward (positive to negative) directions. While we are successfully and consistently able to drive the system from superconducting to normal state and vice versa, we observe slight hysteresis with gate voltage sweeps as it approaches the transition voltage. With an increase in the bias current, the gate voltage required for the transition is higher and the hysteresis becomes more prominent. This could arise as a consequence of charge pinning due to surface inhomogeneities in the thin film. The range over which the quasi-normal state exists broadens with increase in the bias current which may be attributed to inhomogeneous superconducting state at higher currents or intrinsic thermal excitation in the sample and is not due to phase dynamics in the superconductor. Such scaling of the area under the hysteresis curve with bias current makes our device a potential candidate for cryogenic memory systems.[20,47] However, the hysteresis may weaken in thinner films.[48] When the bias current is set to a relatively large value of 150 μA, the system does not achieve the superconducting state (Figure 3d) within the limits of gate voltage allowed by the SiO_2 dielectric.

In order to examine the dependence of gating effect on the bridge dimensions and probe the device scalability to nanoregime, we now present results for the NB device with thickness $t = 7$ nm ($t < \xi_{GL}$). Here, the aspect ratio $w/l = 1/10$ was kept the same as that of the μB. The resistance versus temperature curve in Figure 4a shows a superconducting transition close to 12 K. However, the $I-V$ characteristics show an additional normal metal behavior with finite resistance at 4.2 K (inset of Figure 4a). This appears to be the result of the edge disorder caused by Ar ion milling and the concomitant degradation of the nanowire causing a small drop in the T_c. (We expect a sharper $I-V$ characteristic at lower temperatures) Nevertheless, in these NBs we observe a transition in the I_c-like feature with gate bias similar to that of the μB device discussed previously. On biasing with a constant current of 10 μA and scanning the gate voltage, the NB recovers the superconducting state with a much broader hysteresis (Figure 4c) possibly due to increased charge pinning effects. The ER in this case is nearly 1400%, which is extremely large but finite since the NB does not transition to a completely superconducting state at 4.2 K. We further note the absence of retrapping currents[49] in all of our devices, as seen via $I-V$ characteristics, that is, symmetric in both forward and backward sweeps (Figure 1c and Figure 4a). This observation is in contrast with previous works[20,21,26] and suggests the role of symmetric flux pinning edges.

Our experiments on both μB and NB devices demonstrate a robust coupling of I_c to gate-voltage exhibiting an infinite (large) ER in μB (NB). Despite the T_c drop in the NB on account of an additional disorder, the qualitative effects reported herein remain the same as for the μB thereby demonstrating their scalability for technological applications. Furthermore, the larger hysteresis in the NB should be beneficial for cryogenic memory devices. The gate voltage required to control the superconductor-normal state transition can be brought down significantly, by engineering the oxide layer thickness, to values comparable with the contemporary silicon technology. Finally, we note that similar measurements, presented in the Supporting Information on five different

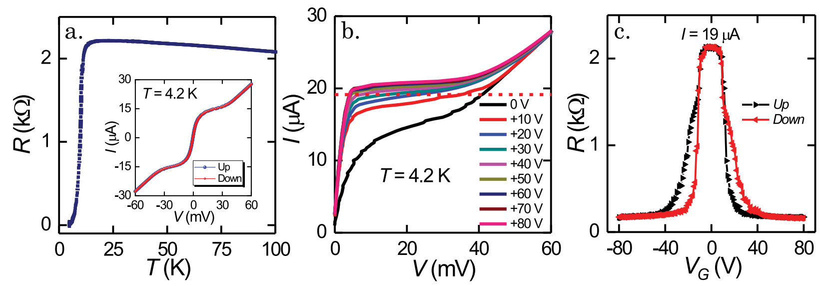

Figure 4. Gate-voltage-control of the NB at 4.2 K. (a) Resistance versus temperature. Inset shows the $I-V$ characteristics without any gate bias (both forward and backward scans). (b) $I-V$ characteristics at different gate voltages (c) Resistance versus V_G at a fixed bias current of 19 μA.

devices with the same aspect ratio, find essentially the same effects as discussed above.

Mechanism and Discussion. We now discuss a plausible mechanism for the observed enhancement in the I_c. Depending on the sample details, such as physical dimensions,[40,41,50] grains, and so on, I_c can be determined by a variety of processes such as critical pair-breaking,[41,51,52] superconducting weak links,[53] an intrinsic proximity effect,[54] and surface vortex (flux) nucleation and flow.[29,30,32] For a homogeneous type II superconductor with t larger than or comparable to ξ, it becomes energetically favorable for vortices nucleating at one edge to move across to the other at large enough currents. This instability of the vortex system then determines the I_c[29,30,32−35,53] and has been the basis for understanding experiments including magnetic field-induced enhancement in I_c of bent superconductors.[34]

Working under the assumption that the vortex instability mechanism discussed above determines the critical current I_c in our films, an applied gate voltage can influence I_c by changing the vortex surface barrier.[29,31] This appears consistent with two key features. First, our experimental observation is that although I_c is affected, critical temperature remains unaltered. A change in vortex surface barrier should not alter critical temperature. Second, the expectation is that electric field is screened over atomic length scales in our high-carrier density superconductor.[16] The gate voltage, therefore, drops largely over the interfaces causing strong interfacial electric fields. The latter should give rise to an interfacial Rashba spin−orbit interaction (SOI) parametrized by $\alpha \propto V_G$. We hypothesize that the ensuing interfacial SOI contributes an amount $\sim\alpha^2 \propto V_G^2$ to the vortex surface barrier and discuss its origin further in the Supporting Information. The vortex surface barrier, and thus the change in critical current, is therefore bipolar. In this manner, we are able to explain all of the key features of our experiments with the caveat that our reasonable sounding hypotheses need to be examined via further theoretical and experimental analyses.

In our considerations above, we have assumed a homogeneous superconducting state consistent with existing experimental evidence for samples similar to ours.[36] Finally, a possible role of magnetic impurities in determining the electric-field-induced vortex pinning in our devices cannot be ruled out.[55] As detailed in the Supporting Information, we have also observed similar gating effects in NbN/GdN bilayer films, where the ferromagnetic GdN layer may play a role via exchange-coupling to the superconducting NbN layer.

CONCLUSION

We have demonstrated gate-voltage-induced enhancement by up to 30% in I_c of NbN-based superconducting bridges. We have put forward a qualitative plausible model that explains our experiments in terms of gate-voltage-controlled surface pinning of vortices. Capitalizing on this voltage control, we demonstrate infinite electroresistance and hysteretic resistance variation in our devices making them promising candidates for logic and memory applications. Our work thus provides fundamental new insights into the field-effect in superconductors, paving the way for even larger voltage-controlled enhancement of superconducting properties and developing novel low-dissipation computing paradigms.

ASSOCIATED CONTENT

Supporting Information

The Supporting Information is available free of charge at https://pubs.acs.org/doi/10.1021/acs.nanolett.0c03547.

Results of measurements on additional devices of NbN and NbN/GdN bilayers; further details of the proposed theoretical model for the mechanism (PDF)

AUTHOR INFORMATION

Corresponding Authors

Mirko Rocci − *Francis Bitter Magnet Laboratory and Plasma Science and Fusion Center, Massachusetts Institute of Technology, Cambridge, Massachusetts 02139, United States; NEST, Istituto Nanoscienze-CNR and Scuola Normale Superiore, I-56127 Pisa, Italy*; Email: rocci@mit.edu

Jagadeesh S. Moodera − *Francis Bitter Magnet Laboratory and Plasma Science and Fusion Center and Department of Physics, Massachusetts Institute of Technology, Cambridge, Massachusetts 02139, United States*; Email: moodera@mit.edu

Dhavala Suri − *Francis Bitter Magnet Laboratory and Plasma Science and Fusion Center, Massachusetts Institute of Technology, Cambridge, Massachusetts 02139, United States*; orcid.org/0000-0003-0085-7648; Email: dmsuri@mit.edu

Authors

Akashdeep Kamra − *Center for Quantum Spintronics, Department of Physics, Norwegian University of Science and Technology, NO-7491 Trondheim, Norway*

Gilvânia Vilela − *Francis Bitter Magnet Laboratory and Plasma Science and Fusion Center, Massachusetts Institute of Technology, Cambridge, Massachusetts 02139, United States; Física de Materiais, Universidade de Pernambuco, Recife 50720-001, Brazil*

https://dx.doi.org/10.1021/acs.nanolett.0c03547
Nano Lett. 2021, 21, 216−221

Yota Takamura − *School of Engineering, Tokyo Institute of Technology, Tokyo 152-8550, Japan*
Norbert M. Nemes − *GFMC, Departamento de Física de Materiales, Universidad Complutense de Madrid, E-28040 Madrid, Spain*
Jose L. Martinez − *Instituto de Ciencia de Materiales de Madrid, C.S.I.C., Cantoblanco, E-28049 Madrid, Spain*
Mar Garcia Hernandez − *Instituto de Ciencia de Materiales de Madrid, C.S.I.C., Cantoblanco, E-28049 Madrid, Spain*

Complete contact information is available at:
https://pubs.acs.org/10.1021/acs.nanolett.0c03547

Author Contributions

◆M.R. and D.S. contributed equally to this work.

Notes

The authors declare no competing financial interest.

■ ACKNOWLEDGMENTS

Authors thank A. K. Saydjari, Prof. Jacobo Santamaria, Prof. Carlos Leon, Morten Amundsen, and Marius Kalleberg Hope for fruitful discussions. M.R. was supported by the Marie Skłodowska-Curie Grant Agreement EuSuper No. 796603 under the European Union's Horizon 2020 research and innovation program. D.S. was supported by CIQM-NSF DMR-1231319, NSF Grant DMR1700137, and ONR Grant N00014-16-1-2657. Research at MIT was supported by NSF Grant DMR1700137, ONR Grant N00014-16-1-2657, and ARO grant W911NF1920041. A.K. acknowledges financial support from the Research Council of Norway through its Centers of Excellence funding scheme, project 262633, "QuSpin". G.V. was supported by ARO Grant W911NF1920041, Brazilian agencies CAPES (Gilvania Vilela/POS-DOC-88881.120327/2016-01), FACEPE (APQ-0565-1.05/14), CNPq and UPE (PFA/PROGRAD/UPE 04/2017). M.G.H., J.L.M., and N.M.N. were supported by Spanish MICIN Grants MAT2017-87134- C02 and MAT2017-84496-R.

■ REFERENCES

(1) Bonfiglioli, G.; Coen, E.; Malvano, R. Modulation of Conductivity by Surface Charges in Metals. *Phys. Rev.* **1956**, *101*, 1281−1284.
(2) Bonfiglioli, G.; Malvano, R. Surface States in Metals. *Phys. Rev.* **1959**, *115*, 330−335.
(3) Glover, R. E.; Sherrill, M. D. Changes in Superconducting Critical Temperature Produced by Electrostatic Charging. *Phys. Rev. Lett.* **1960**, *5*, 248−250.
(4) Ahn, C. H.; Triscone, J.-M.; Mannhart, J. Electric field effect in correlated oxide systems. *Nature* **2003**, *424*, 1015.
(5) Xi, X. X.; Doughty, C.; Walkenhorst, A.; Kwon, C.; Li, Q.; Venkatesan, T. Effects of field-induced hole-density modulation on normal-state and superconducting transport in $YBa_2Cu_3O_{7-x}$. *Phys. Rev. Lett.* **1992**, *68*, 1240−1243.
(6) Frey, T.; Mannhart, J.; Bednorz, J. G.; Williams, E. J. Mechanism of the electric-field effect in the high-T_c cuprates. *Phys. Rev. B: Condens. Matter Mater. Phys.* **1995**, *51*, 3257−3260.
(7) Sajadi, E.; Palomaki, T.; Fei, Z.; Zhao, W.; Bement, P.; Olsen, C.; Luescher, S.; Xu, X.; Folk, J. A.; Cobden, D. H. Gate-induced superconductivity in a monolayer topological insulator. *Science* **2018**, *362*, 922−925.
(8) Costanzo, D.; Jo, S.; Berger, H.; Morpurgo, A. F. Gate-induced superconductivity in atomically thin MoS2 crystals. *Nat. Nanotechnol.* **2016**, *11*, 339−344.
(9) Hanzawa, K.; Sato, H.; Hiramatsu, H.; Kamiya, T.; Hosono, H. Electric field-induced superconducting transition of insulating FeSe thin film at 35 K. *Proc. Natl. Acad. Sci. U. S. A.* **2016**, *113*, 3986−3990.
(10) Wang, J.; Ma, X.-C.; Lu, L.; Jin, A.-Z.; Gu, C.-Z.; Xie, X. C.; Jia, J.-F.; Chen, X.; Xue, Q.-K. Anomalous magnetoresistance oscillations and enhanced superconductivity in single-crystal Pb nanobelts. *Appl. Phys. Lett.* **2008**, *92*, 233119.
(11) Giazotto, F. A boost for quantum computing. *Nat. Phys.* **2015**, *11*, 527−528.
(12) Linder, J.; Robinson, J. W. A. Superconducting spintronics. *Nat. Phys.* **2015**, *11*, 307−315.
(13) Moraru, I. C.; Pratt, W. P.; Birge, N. O. Magnetization-Dependent T_c Shift in Ferromagnet/Superconductor/Ferromagnet Trilayers with a Strong Ferromagnet. *Phys. Rev. Lett.* **2006**, *96*, 037004.
(14) Khaire, T. S.; Pratt, W. P.; Birge, N. O. Critical current behavior in Josephson junctions with the weak ferromagnet PdNi. *Phys. Rev. B: Condens. Matter Mater. Phys.* **2009**, *79*, 094523.
(15) Bergeret, F. S.; Silaev, M.; Virtanen, P.; Heikkilä, T. T. Colloquium: Nonequilibrium effects in superconductors with a spin-splitting field. *Rev. Mod. Phys.* **2018**, *90*, 041001.
(16) Lipavský, P.; Koláček, J.; Morawetz, K. In *Nanoscience and Engineering in Superconductivity*; Moshchalkov, V., Woerdenweber, R., Lang, W., Eds.; Springer Berlin Heidelberg: Berlin, Heidelberg, 2010; pp 281−297.
(17) Cavalleri, A. Photo-induced superconductivity. *Contemp. Phys.* **2018**, *59*, 31−46.
(18) Demsar, J. Non-equilibrium Phenomena in Superconductors Probed by Femtosecond Time-Domain Spectroscopy. *J. Low Temp. Phys.* **2020**, *201*, 676.
(19) London, F.; London, H. Supraleitung und diamagnetismus. *Physica* **1935**, *2*, 341−354.
(20) De Simoni, G.; Paolucci, F.; Solinas, P.; Strambini, E.; Giazotto, F. Metallic supercurrent field-effect transistor. *Nat. Nanotechnol.* **2018**, *13*, 802−805.
(21) De Simoni, G.; Paolucci, F.; Puglia, C.; Giazotto, F. Josephson Field-Effect Transistors Based on All-Metallic Al/Cu/Al Proximity Nanojunctions. *ACS Nano* **2019**, *13*, 7871−7876.
(22) De Simoni, G.; Puglia, C.; Giazotto, F. Niobium Dayem nano-bridge Josephson gate-controlled transistors. *Appl. Phys. Lett.* **2020**, *116*, 242601.
(23) Puglia, C.; De Simoni, G.; Ligato, N.; Giazotto, F. Vanadium gate-controlled Josephson half-wave nanorectifier. *Appl. Phys. Lett.* **2020**, *116*, 252601.
(24) Piatti, E.; Romanin, D.; Gonnelli, R. S.; Daghero, D. Anomalous screening of an electrostatic field at the surface of niobium nitride. *Appl. Surf. Sci.* **2018**, *461*, 17−22.
(25) Rocci, M.; De Simoni, G.; Puglia, C.; Esposti, D. D.; Strambini, E.; Zannier, V.; Sorba, L.; Giazotto, F. Gate-Controlled Suspended Titanium Nanobridge Supercurrent Transistor. *ACS Nano* **2020**, *14*, 12621−12628.
(26) Paolucci, F.; De Simoni, G.; Strambini, E.; Solinas, P.; Giazotto, F. Ultra-Efficient Superconducting Dayem Bridge Field-Effect Transistor. *Nano Lett.* **2018**, *18*, 4195−4199.
(27) Alegria, L. D.; Bøttcher, C. G.; Saydjari, A. K.; Pierce, A. T.; Lee, S. H.; Harvey, S. P.; Vool, U.; Yacoby, A. *High-Energy Quasiparticle Injection in Mesoscopic Superconductors*. 2020, 2005.00584, arXiv, https://arxiv.org/abs/2005.00584 (accessed 2020−06−08).
(28) Ritter, M. F.; Fuhrer, A.; Haxell, D. Z.; Hart, S.; Gumann, P.; Riel, H.; Nichele, F. *A superconducting switch actuated by injection of high energy electrons*. 2020, 2005.00462, arXiv, https://arxiv.org/abs/2005.00462 (accessed 2020−06−08).
(29) Shmidt, V. V. Critical Currents in Superconductors. *Sov. Phys. Uspekhi* **1970**, *13*, 408−409.
(30) Shmidt, V. V. The Critical Current in Superconducting Films. *Sov. Phys. JETP* **1970**, *30*, 1137.
(31) Bean, C. P.; Livingston, J. D. Surface Barrier in Type-II Superconductors. *Phys. Rev. Lett.* **1964**, *12*, 14−16.

(32) Aslamazov, L. G.; Larkin, A. I. Josephson effect in wide superconducting bridges. *Sov. Phys. JETP* **1975**, *41*, 381.
(33) Mawatari, Y.; Yamafuji, K. Critical current density in thin films due to the surface barrier. *Phys. C* **1994**, *228*, 336−350.
(34) Ilin, K.; Henrich, D.; Luck, Y.; Liang, Y.; Siegel, M.; Vodolazov, D. Y. Critical current of Nb, NbN, and TaN thin-film bridges with and without geometrical nonuniformities in a magnetic field. *Phys. Rev. B: Condens. Matter Mater. Phys.* **2014**, *89*, 184511.
(35) Clem, J. R.; Berggren, K. K. Geometry-dependent critical currents in superconducting nanocircuits. *Phys. Rev. B: Condens. Matter Mater. Phys.* **2011**, *84*, 174510.
(36) Romestain, R.; Delaet, B.; Renaud-Goud, P.; Wang, I.; Jorel, C.; Villegier, J.-C.; Poizat, J.-P. Fabrication of a superconducting niobium nitride hot electron bolometer for single-photon counting. *New J. Phys.* **2004**, *6*, 129−129a.
(37) Tinkham, M. *Introduction to Superconductivity*; Dover Publications, Inc.: New York, 2004.
(38) Komenou, K.; Yamashita, T.; Onodera, Y. Energy gap measurement of niobium nitride. *Phys. Lett. A* **1968**, *28*, 335−336.
(39) Chockalingam, S. P.; Chand, M.; Jesudasan, J.; Tripathi, V.; Raychaudhuri, P. Superconducting properties and Hall effect of epitaxial NbN thin films. *Phys. Rev. B: Condens. Matter Mater. Phys.* **2008**, *77*, 214503.
(40) Pearl, J. Current Distribution in Superconducting Films Carrying Quantized Fluxoids. *Appl. Phys. Lett.* **1964**, *5*, 65−66.
(41) Romijn, J.; Klapwijk, T. M.; Renne, M. J.; Mooij, J. E. Critical pair-breaking current in superconducting aluminum strips far below T_c. *Phys. Rev. B: Condens. Matter Mater. Phys.* **1982**, *26*, 3648−3655.
(42) Moodera, J. S.; Kinder, L. R.; Wong, T. M.; Meservey, R. Large Magnetoresistance at Room Temperature in Ferromagnetic Thin Film Tunnel Junctions. *Phys. Rev. Lett.* **1995**, *74*, 3273−3276.
(43) Moodera, J. S.; Nassar, J.; Mathon, G. Spin-tuneling in ferromagnetic junctions. *Annu. Rev. Mater. Sci.* **1999**, *29*, 381−432.
(44) Žutić, I.; Fabian, J.; Das Sarma, S. Spintronics: Fundamentals and applications. *Rev. Mod. Phys.* **2004**, *76*, 323−410.
(45) Fert, A. Nobel Lecture: Origin, development, and future of spintronics. *Rev. Mod. Phys.* **2008**, *80*, 1517−1530.
(46) Giazotto, F.; Heikkilä, T. T.; Luukanen, A.; Savin, A. M.; Pekola, J. P. Opportunities for mesoscopics in thermometry and refrigeration: Physics and applications. *Rev. Mod. Phys.* **2006**, *78*, 217−274.
(47) Gingrich, E. C.; Niedzielski, B. M.; Glick, J. A.; Wang, Y.; Miller, D. L.; Loloee, R.; Pratt, W. P., Jr; Birge, N. O. Controllable 0-p Josephson junctions containing a ferromagnetic spin valve. *Nat. Phys.* **2016**, *12*, 564−567.
(48) Tinkham, M.; Free, J. U.; Lau, C. N.; Markovic, N. Hysteretic $I - V$ curves of superconducting nanowires. *Phys. Rev. B: Condens. Matter Mater. Phys.* **2003**, *68*, 134515.
(49) Courtois, H.; Meschke, M.; Peltonen, J. T.; Pekola, J. P. Origin of hysteresis in a proximity Josephson junction. *Phys. Rev. Lett.* **2008**, *101*, 067002.
(50) Korneeva, Y. P.; Vodolazov, D. Y.; Semenov, A. V.; Florya, I. N.; Simonov, N.; Baeva, E.; Korneev, A. A.; Goltsman, G. N.; Klapwijk, T. M. Optical Single-Photon Detection in Micrometer-Scale NbN Bridges. *Phys. Rev. Appl.* **2018**, *9*, 064037.
(51) Bardeen, J. Critical Fields and Currents in Superconductors. *Rev. Mod. Phys.* **1962**, *34*, 667−681.
(52) De Gennes, P. G. *Superconductivity of Metals and Alloys*; Advanced book classics; Perseus: Cambridge, MA, 1999.
(53) Likharev, K. K. Superconducting weak links. *Rev. Mod. Phys.* **1979**, *51*, 101−159.
(54) Charaev, I.; Silbernagel, T.; Bachowsky, B.; Kuzmin, A.; Doerner, S.; Ilin, K.; Semenov, A.; Roditchev, D.; Vodolazov, D. Y.; Siegel, M. Proximity effect model of ultranarrow NbN strips. *Phys. Rev. B: Condens. Matter Mater. Phys.* **2017**, *96*, 184517.
(55) Mironov, S.; Buzdin, A. Spontaneous Currents in Superconducting Systems with Strong Spin-Orbit Coupling. *Phys. Rev. Lett.* **2017**, *118*, 077001.

https://dx.doi.org/10.1021/acs.nanolett.0c03547
Nano Lett. 2021, 21, 216−221